Electronic Supplementary Material (ESI) for Journal of Materials Chemistry A.

Layered Inorganic-Organic Hybrid Material Based on Reduced Graphene Oxide and α-$Ni(OH)_2$ for High Performance Supercapacitor Electrodes

*Sourav Bag and C. Retna Raj**

Functional Materials and Electrochemistry Laboratory
Department of Chemistry
IIT Kharagpur
Kharagpur 721302, West Bengal, India

Figure S1. FTIR spectral profile of GO, free $Ni(OH)_2$, rGO and rGO/α-$Ni(OH)_2$

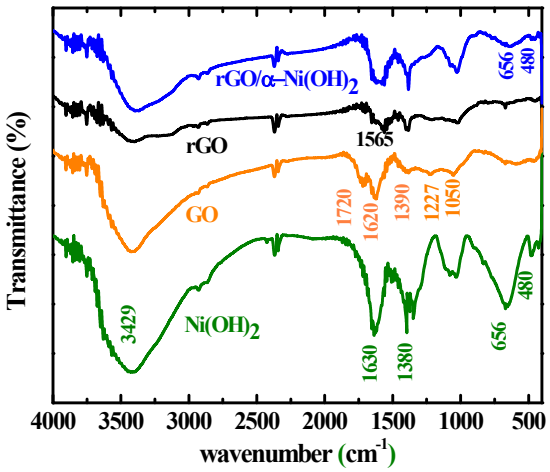

The FTIR spectral profile of rGO/α-$Ni(OH)_2$ shows a broad band around 3429 cm^{-1} corresponding to the stretching frequency of hydroxyl group of nickel hydroxide hydrogen bonded to water molecules in the interlamellar space. The characteristic bands for the IR-active modes of α-$Ni(OH)_2$ were observed at 480 (ν_{Ni-O}) and 656 (δ_{Ni-O-H}) cm^{-1}.[1, 2] The band at 1630 cm^{-1} is assigned to the bending mode of interlayer water molecule.[3] In the case of GO, the broad band ~ 3430 cm^{-1} is assigned to the stretching of -OH group. The other peaks are due to stretching of oxygen functionalities such as C=O (1720 cm^{-1}), C-OH (ν_{C-OH} at 1390 cm^{-1}), epoxy C-O-C (ν_{C-O} at 1227 cm^{-1}), alkoxy C-O (1050 cm^{-1}) groups.[4,5] The band at 1620 cm^{-1} is due to graphitic domain ($\nu_{C=C}$) of the carbon framework.[5] The peak at 1565 cm^{-1} for rGO is due to the skeletal vibration of rGO sheet.[6]

Figure S2. FESEM image (a, b) and EDS line scale analysis (c, d) for the rGO/α-$Ni(OH)_2$ hybrid material.

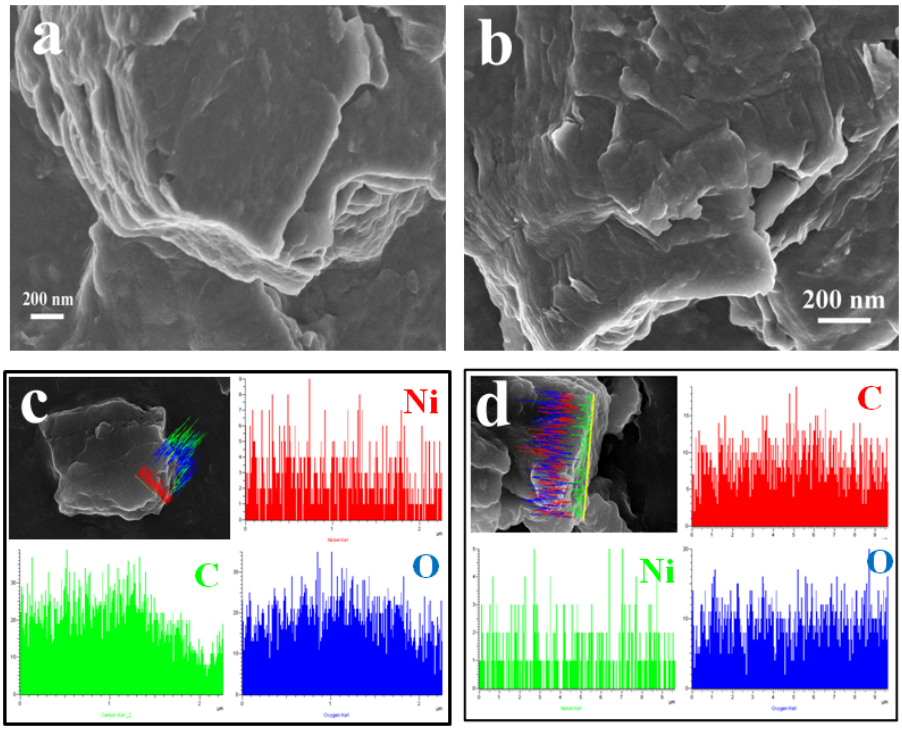

The FESEM image (a, b) show the layer structure of the hybrid material whereas the mapping through the line scan reveals that the layers are made of Nickel hydroxide and rGO sheets.

Figure S3. TEM image of free α-$Ni(OH)_2$.

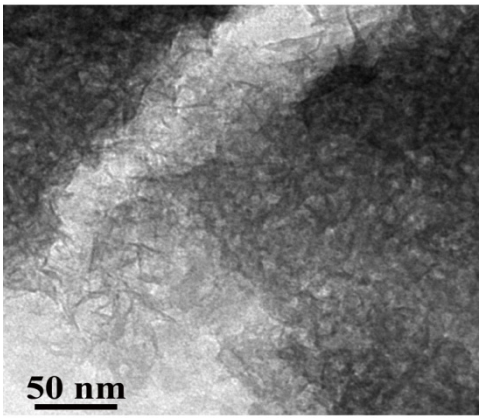

Figure S4. (A) XRD pattern and (B) TEM measurement of rGO-$Ni(OH)_2$ synthesized in absence of D-glucose.

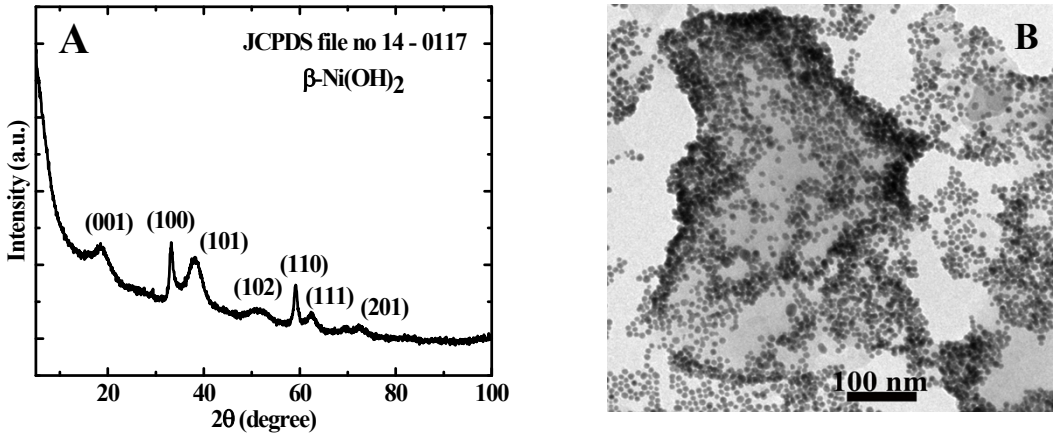

The XRD pattern clearly reveals the β phase of the $Ni(OH)_2$ nanoparticles. The edge of the rGO contains high amount of $Ni(OH)_2$ as the amount of oxygen functionalities is higher at the edge of the GO**.** The β-$Ni(OH)_2$ distributed over the rGO sheets have an average particle size of 10 nm.

Figure S5. TGA of free $Ni(OH)_2$ and rGO/α-$Ni(OH)_2$ hybrid material.

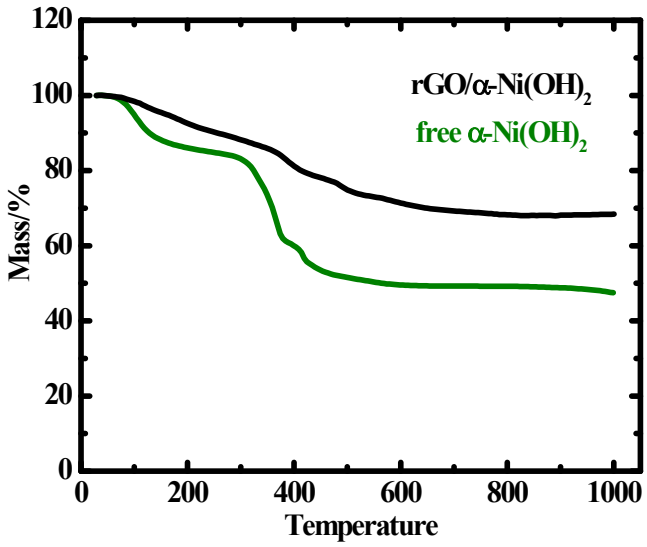

The initial loss of mass is ascribed to the loss of water including those intercalated between the $Ni(OH)_2$ layers. The mass loss around 200-450 ^{O}C can be ascribed to the phase transition of $Ni(OH)_2$ to NiO.[7] The hybrid material is thermally more stable than the free $Ni(OH)_2$. Though the loss of intercalated water molecule of α-$Ni(OH)_2$ occurs almost at same temperature, the phase transition of $Ni(OH)_2$ to NiO in the hybrid occurs at high temperature and the mass loss is rather slow.

Figure S6. (A) Rate capability and (B) cyclic performance of rGO/α-$Ni(OH)_2$ hybrid material at different current density.

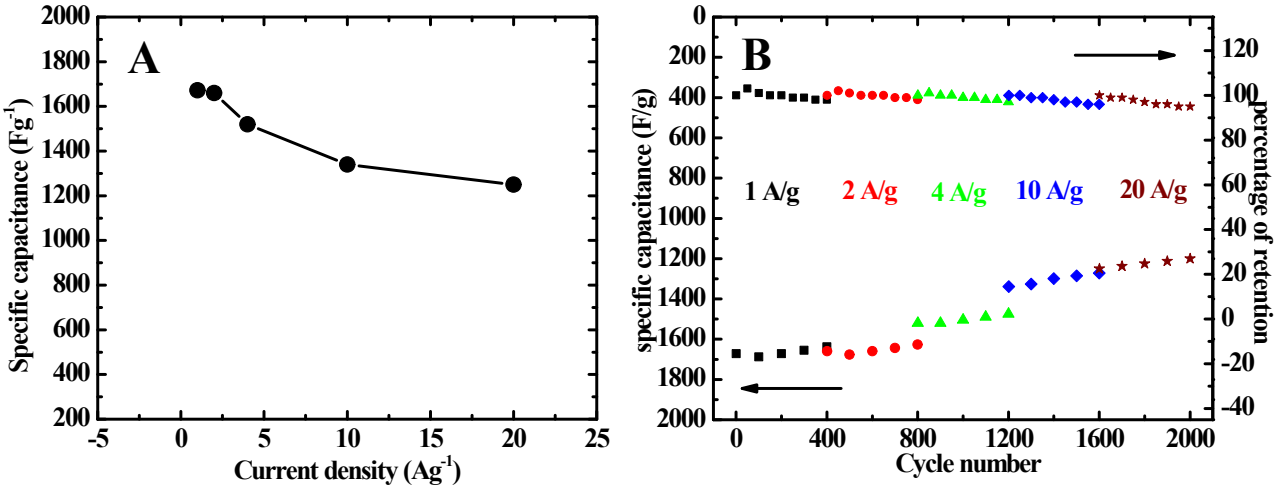

Figure S7. Equivalent circuit and the electrochemical impedance parameters obtained from the Nyquist plot.

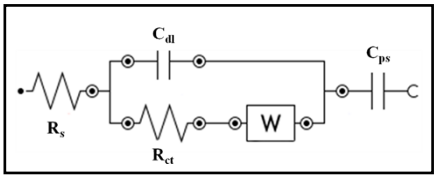

Potential (V)	R_{ct} (ohm)	W (mMho)	C_{dl} (µF)	C_{ps} (mF)
0.3	470	1.60	411	874
0.4	260	2.25	431	89.3
0.5	20.7	22.4	659	275

Figure S8. (A) Plot illustrating the frequency-dependent specific capacitance of rGO/α-$Ni(OH)_2$ electrode at different potential. (B) voltammetric profile of rGO/α-$Ni(OH)_2$ at different scan rate.

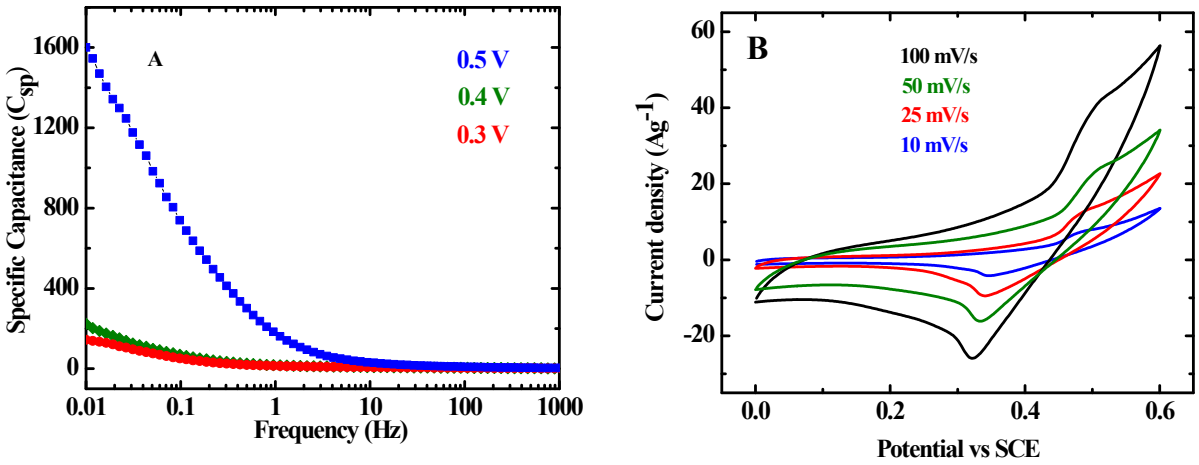

Figure S9. Electrochemical impedance spectroscopic (EIS) study of rGO/α-$Ni(OH)_2$ after 1000 charge discharge cycles at 0.5 V potential.

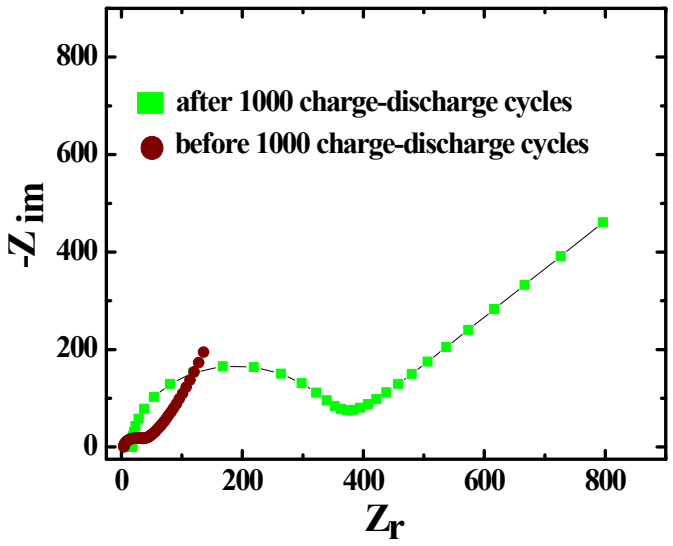

Figure S10. Schematic illustration of the asymmetric supercapacitor device.

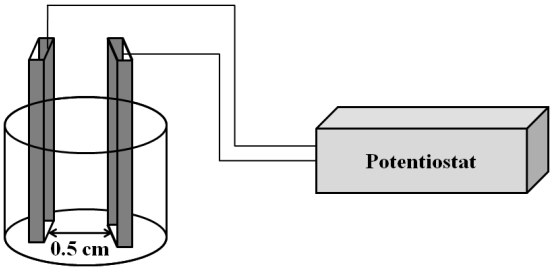

The electrodes for the supercapacitor device were prepared by following the same procedure as the three electrode cell experiments. The mass loading on each electrode was controlled by maintaining the charge balance of the electrode. The charge accumulated in the cathode (Q_c) should be equal to the anodic charge (Q_a).

To maintain the equal charge balance, $Q_c=Q_a$,

$$m_c Cs_c \Delta V_c = m_a Cs_a \Delta V_a$$

where m_c and m_a are the mass of electrode material in the cathode and anode, respectively. Cs is the specific capacitance of the electrode material. ΔV is the potential window for charge discharge of the corresponding electrode material in three electrode system.

$$m_c/m_a = Cs_a/Cs_c$$

The loaded mass of the active layered hybrid material (m_c) on the Ni foam is ~0.5 mg. The specific capacitance of the rGO/α-$Ni(OH)_2$ is 1761 F/g and the rGO is 126 F/g. The amount of rGO taken for the anode is 7 mg. The two electrodes were kept in a beaker like cell and the distance between the two electrodes were maintained at the distance of 0.5 cm. KOH (1 M) was used as electrolyte.

Figure S11. Repeated 500 charge-discharge cycles of the asymmetric supercapacitor device (ASD) at a current density of 20 A g^{-1}.

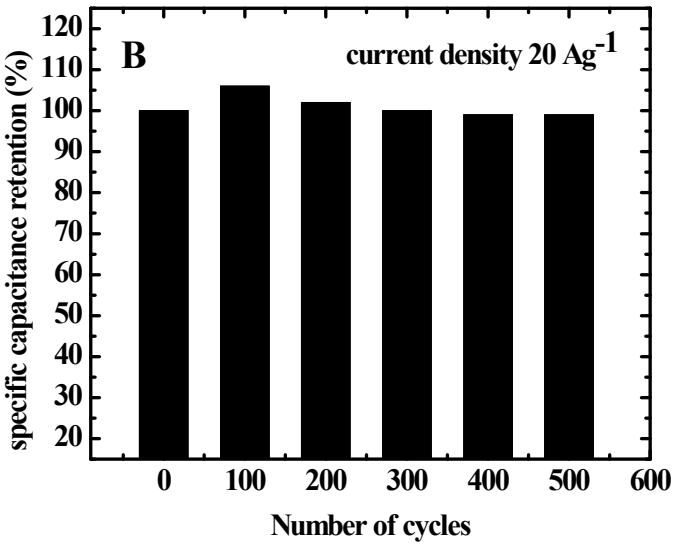

Table S 1

	Synthetic route	**morphology**	**Specific capacitance**	**Current collector**	**recyclability**
J. Mater. Chem., 2012, ***22***, 11146.	$Ni(OAc)_2$ refluxed at100^oC for 4 h with PVP dispersed graphene	$Ni(OH)_2$ nanoflakes over rGO	1828 Fg^{-1} at 1 Ag^{-1}	Nickel foam	84.5% after 1000 cycles at 6Ag^{-1}
Chem. Commun., 2012, ***48***, 2773.	hexamethylenetetramine (HMT, $C_6H_{12}N_4$) put in autoclave	nanoflake, forming a hierarchical network-like structure.	1026 F g^{-1} at 5.7 A g^{-1} 1760.72 F g^{-1} at a scan rate of 5 mV s^{-1}	Ni foam	100% (from repeated cv)
J. Mater. Chem., 2012, ***22***, 11494.	reflux with rGO and $NiCl_2$, pH 9.5 by NH_3	$Ni(OH)_2$ nanosheet	2194 F g^{-1} could be obtained at 2 mV s^{-1}	Ni foam	95.7% after 2000 cv scan
J. Am. Chem. Soc., 2010, ***132***, 7472.	GO and aqueous Ni precursor in DMF and heated at 80^oC. Then put into autoclave.	nanoplate	1335 F/g at 2.8 A/g	Ni foam	100% after 2000 cycles at 28.6A/g
J. Phys. Chem. B 2013, ***117***, 1616.	Electrodepostion by GO and Ni salt	Flower-like	1404 F g^{-1} at 2 A g^{-1},	Stainless steel	89.8% after 1000 cycles at 20A/g
J. Electrochem. Soc., 2013, ***160***, A98.	Autoclave rGO and Ni salt	nanowire	1700 F/g at 1A/g	Ni foam	90% after 5000 cycles at 4.5A/g
Ind. Eng. Chem. Res. 2012, ***51***, 9973.	4-sulfobenzenediazonium tetrafluoroborate functionalized rGO was reacted with a mixture of Ni salt and KOH by grounding it in a morter pestle as a solid state reaction approach	Small particle	1568 F g^{-1} at 4 A g^{-1}	Ni foam	75% after 1000 cycles at 4 A/g

Chem. Mater., 2011, ***23***, 4810.	1. CNT Graphene composite 2.$Ni(OH)_2$ coating by electrodeposition	Uniform coating of $Ni(OH)_2$ over CNT-Gr	1384 F/g at a scan rate of 5 mV/s	CNT Gr nanostruct -ure	96% after 20000 cycles at 21.5A/g
J. Mater. Chem. A, 2013, ***1***, 478.	one-step solvothermal route using ethylene glycol as a solvent. ($Ni(OH)_2$ /CoO/ rGO)	Flower-like	1317 F g^{-1} at a current density of 2 A g^{-1}	Ni foam	84.5% after 2000 cycles at 5mV/s
ACS Appl. Mater. Interfaces, 2013, ***5***, 5443.	Autoclave (Ni Al Double layer hydroxide over CNT and rGO)	Hexagonal n flower plate	1404 F/g at 5 mV/s,	Ni foam	96.5% after 1000 cycles
Chem. Eur. J., 2013, ***19***, 7118.	Hydrolysis of $Ni(NO_3)_2$ in NMP autoclave	particle	1250.3 Fg^{-1}	Ni foam	95% after 1000 cycles
Adv. Funct. Mater., 2012, ***22***, 2632.	Microwave heating	Flower-like	1735 F g^{-1} (218 F/g in 2 electrode process)	Ni foam	94.3% after 3000 cycles
Nano Res., 2012, ***5***, 11.	Hydrolysis of graphene and Ni nitrate	Flower-like	1087.9 F/g at 1 A/g	Ni foam	90% after 2000 cycles
Nano Res., 2011, ***4***, 729.	Gr $Ni(OH)_2$ and Gr RuO_2 device, two step solution phase approach approach	nanoplate	900 F/g at 2A/g (Gr $Ni(OH)_2$)	Ni foam	92% after 5000 cycles at10A/g
Microchim Acta, 2012, ***177,*** 103.	Electrodepostion	sphere	Glucose sensing		
Nano Energy, 2013, ***2***, 65.	$Ni(acac)_2$, GO and benzyl alcohol in autoclave	Lamellar layer by layer structure	660.8 Fcm_3	Au foil	Almost 100% after 2000cycles

Journal of Alloys and Compounds, 2013, ***549***, 147.	Gr on Ni foam by CVD. $Ni(OH)_2$ by hydrothermal method	sheet	1440 F/g at 1 A/g	Ni foam	100% after 2000 cycles
Journal of Power Sources, 2013, ***238***, 180e.	microwave-assisted hydrothermal annealing of as prepared $Ni(OH)_2$ and $Co(OH)_2$	particle	215 F/g at 1A/g	graphite	
Journal of Power Sources, 2013, ***222***, 326.	RGO-CNT by CVD then stabilized by SDS and reflux	particle	1235 F/g at 1 A/g	GC	80% after 500 cycle at 10A/g
Journal of Power Sources, 2013, ***221***, 128.	Electrochemical deposition	flower	2217 F/g	graphite	-
Electrochimica Acta 2013, ***94***, 360.	Conversion of GO to rGO and hydrothermal deposition of $Ni(OH)_2$ and $Al(OH)_3$	Thin nanoflakes	1730.2 F g^{-1} at 0.1 A g^{-1}.	Ni foam	99.2% after 500 cycles at 5 A/g
Electrochimica Acta 2012**,** ***81****, 321.*	1.RGO prepared by N_2H_4 2.$Ni(OH)_2$ was precipitated by NaOH	Particle	1482 F/g at 1A/g	Ni foam	81% after 2000 cycles at 10A/g
Chemical Physics Letters 2013**,** ***573***, 41.	Ag was precipitated by UV irradiation with Gr-$Ni(OH)_2$ suspension.	Flower-like	496 F/g at 1 A/g	GC	93% after 500 cycle

Nano Research, 2013, ***6***, 65.	heating a homogeneous aqueous mixtureof graphene oxide (GO), Ni(NO3)2, ammonia and hydrazine at 180 °C for 2 h	plate	~1,327 F/g at 1A/g	Ni foam	95% after 2000 cycles at 16A/g
Chem. Commun., 2011, ***47***, 6305.	In situ synthesis of RGO-$Ni(OH)_2$ in ethylene glycol	Spherical particles	1215F/g at 5mV/s	Ni foam	97.9% after 1000cycle
This work	One step synthesis by using D-glucose as a soft template for α-$Ni(OH)_2$ paper and reducing agent for GO.	Layered structure inorganic organic hybrid material	1671 F/g at 1A/g	Ni foam	81% After 2000 cycles

Table S2

Table summarizing the energy density of nickel hydroxide/nickel oxide or double hydroxide based symmetric/asymmetric supercapacitor devices. Performance of two electrode devices is compared here. Three electrode systems are not considered here.

Journal name	**Specific Capacitance (F/g)**	**Energy density (Wh/kg)**	**Corresponding Power density (kW/kg)**
Adv. Funct. Mater., 2012, ***22***, 2632.	218 at 1mV/s	77.8	0.1747
Nano Res, 2011, ***4***, 729.	160 at 0.5A/g	48	0.23
J. Mater. Chem. A, 2013, ***1***, 13290.	130.2 at 0.2 A g^{-1}	36.46	0.142
J. Power Sources, 2014, ***246***, 371.	105.8 at 2mAcm^{-2}	36.2	0.1006
Nanoscale, 2012, ***4***, 7266.	125.2 Fg^{-1} at 0.88 Ag^{-1}	23.7	0.2842
J. Mater. Chem. A, 2014, ***2***, 4795.	112 F g^{-1} at 1 mA cm^{-2}	35	0.163
J. Mater. Chem., 2012, ***22***, 23114.	99.4 F g^{-1} at 0.5 A g^{-1}	23.32	0.3249
J. Power Sources, 2008, ***185***, 1563.	37F/g	10-20	-

J. Power Sources, 2010, ***193***, 3017.	-	41.65	-
J. Power Sources, 2010, ***195***, 6239.	-	15-20	-
J. Electrochem. Soc., 2006**,** ***153***, A743.	-	40	0.1
J. Soild State Electrochem., 2010, ***14***, 1533.	127 F/g	42.3	0.11
This work	120 at 0.5A/g	44	0.4

References:

1. L. X. Yang, Y. J. Zhu, H. Tong, Z. H. Liang, L. Li, L. Zhang, *Journal of Solid State Chemistry* 2007**,** 180, 2095.
2. M. Rajamathi, P. V. Kamath, *Journal of Power Sources* 1998**,** 70, 118.
3. R. L. Frost, J. T. Kloprogge, Z. Ding, *Spectrochimica Acta Part A* 2002**,** 58, 1657.
4. R. S. Dey, S. Hajra, R. K. Sahu, C. R. Raj, M. K. Panigrahi, *Chem. Commun*., 2012, 48, 1787.
5. Y. Liang, D. Wu, X. Feng, K. Müllen, *Adv. Mater*. 2009, 21, 1679.
6. P. Lian, X. Zhu, S. Liang, Z. Li, W. Yang, H. Wang, *Electrochimica Acta* 2010**,** 55, 3909.
7. S. Chen, J. Duan, Y. Tang, S. Z. Qiao *Chem. Eur. J*. 2013, 19, 7118.